CHEMISTRY
A EUROPEAN JOURNAL

DOI: 10.1002/chem.200800605

Combining G-Quadruplex Targeting Motifs on a Single Peptide Nucleic Acid Scaffold: A Hybrid (3+1) PNA–DNA Bimolecular Quadruplex**

Alexis Paul,[a] Poulami Sengupta,[b] Yamuna Krishnan,[b] and Sylvain Ladame*[a]

Abstract: We describe the first G-quadruplex targeting approach that combines intercalation and hybridization strategies by investigating the interaction of a G-rich petide nucleic acid (PNA) acridone conjugate **1** with a three-repeat fragment of the human telomere **G3** to form a hybrid PNA–DNA quadruplex that mimicks the biologically relevant (3+1) pure DNA dimeric telomeric quadruplex. Using a combination of UV and fluorescence spectroscopy, circular dichroism (CD), and mass-spectrometry, we show that PNA **1** can induce the formation of a bimolecular hybrid quadruplex even at low salt concentration upon interaction with a single-stranded three-repeat fragment of telomeric DNA. However, PNA **1** cannot invade a short fragment of B-DNA even if the latter contains a CCC motif complementary to the PNA sequence. These studies could open up new possibilities for the design of a novel generation of quadruplex ligands that target not only the external features of the quadruplex but also its central core constituted by the tetrads themselves.

Keywords: acridone · circular dichroism · DNA recognition · eptide nucleic acid · quadruplex

Introduction

It has been known for several decades that DNA sequences containing a high density of clustered guanine units are able to adopt four-stranded secondary structures named guanine (G) quadruplexes or tetraplexes in the presence of physiological cations, notably K^+ and Na^+ (Scheme 1).[1] Converging data collected from computer simulation and in vitro have revealed the high prevalence of such G-rich DNA sequences throughout the human genome.[2] Recently, there has been considerable focus on quadruplexes, their cellular functions, and their exploitation for biological intervention towards therapeutics. The most widely studied DNA quadruplexes are those derived from telomeric repeat sequences.[3–6] Biophysical studies on the human telomeric quadru-

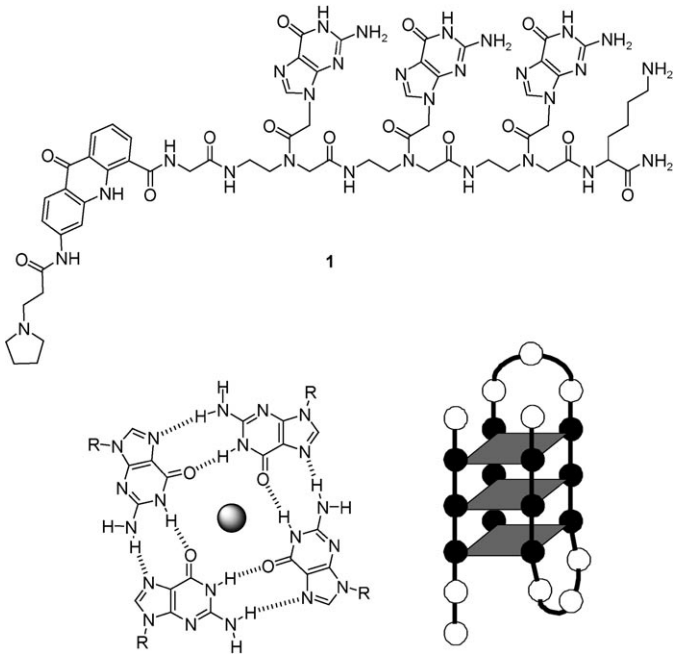

Scheme 1. Top: structure of the first generation acridone–PNA conjugate **1**. Bottom: planar array of four guanine units or a G tetrad (left) and schematic representation of a bimolecular (3+1) G-quadruplex structure (right) determined by NMR spectroscopy by Patel and co-workers.[16].

[a] A. Paul, Dr. S. Ladame
Institut de Science et d'Ingénierie
Supramoléculaires (ISIS), Université Louis Pasteur
CNRS UMR 7006, 8, Allée Gaspard Monge
67083 Strasbourg Cédex (France)
Fax: (+33) 3902-45115
E-mail: s.ladame@isis.u-strasbg.fr

[b] P. Sengupta, Dr. Y. Krishnan
National Centre for Biological Sciences
TIFR, Bellary Road, Bangalore, 560065 (India)

[**] 1 PNA + 1 DNA = (3+1) quadruplex

plex have provided valuable insight into its structural and dynamic properties.[3]

NMR spectroscopic and X-ray crystallographic studies of the intramolecular quadruplex formed from four human telomeric repeats (GGGTTA) have revealed that it is highly polymorphic.[4] Several lines of evidence link G quadruplexes with telomere maintenance[5], given that telomeric DNA in the quadruplex form is not a competent substrate for telomerase.[6] Telomerase is crucial for immortality in most human cancers, and therefore ligand-induced quadruplex stabilization in telomeric DNA has potential as an anticancer therapeutic strategy.[7] Thus far, strategies for targeting quadruplexes include small molecules,[8] complementary oligonucleotides,[9] or engineered DNA-binding proteins.[10] An original approach was also recently reported that uses an anthracene/diethylene triamine conjugate to induce intramolecular parallel quadruplex formation from single-stranded DNA through stacking of the anthracene moiety onto the external G tetard and invasion of the central ion channel by the triamine side chain.[11] Peptide nucleic acid (PNA) is a synthetic mimic of DNA in which the negatively charged phosphate backbone is replaced by a neutral polyamide backbone, thus allowing it to hybridise in a sequence specific manner and with high affinity to either DNA or RNA. Recently, it has been shown that carefully designed G-rich PNA oligomers were also capable of forming PNA_4 quadruplexes[12], hybrid PNA_2–DNA_2,[13] PNA_2—DNA,[14] or $(PNA–DNA\ chimeras)_4$[15] tetramolecular and trimolecular quadruplexes.

A recent NMR spectroscopic study reported an unprecedented structure of a DNA fragment of the human telomeric region containing three G-rich repeats, namely, d(GGGTTAGGGTTAGGGT) in a solution of sodium cations.[16] An asymmetric dimeric quadruplex was formed in which the G-tetrad core involved all three G tracts of one of the strands and the G tract at the 3′-end of the second strand. The three-repeat sequence could also associate with the solitary G-rich unit d(GGGTTA) to form a bimolecular complex called the (3+1) assembly. We, therefore, reasoned that this bimolecular (3+1) structure could represent the basis of a promising new design strategy for G-quadruplex stabilizing ligands. These ligands could combine on a single scaffold, binding elements that target simultaneously the central core of the G-quadruplex structure and key external features, that is, a G-rich PNA strand attached to a quadruplex binding platform. The G-rich PNA region could hybridize with the G-rich DNA clusters to form three hybrid G tetrads, whereas the quadruplex binding platform could stack on the resultant terminal G tetrad of the hybrid quadruplex core. We chose an acridone as our DNA-binding platform as it is a well-characterized G-tetrad end-stacker[17] for which high quadruplex versus duplex DNA discrimination capabilities have been demonstrated when appending appropriate side chains (e.g., 3-pyrrolidine propionamide).

We report herein the synthesis of ligand **1**, a G-rich PNA–acridone conjugate (Scheme 1), and demonstrate the successful targeting of a three-repeat fragment of human telomeric DNA by the formation of a bimolecular (3+1) hybrid quadruplex.

Results and Discussion

Design and synthesis: We designed PNA–acridone conjugate **1** such that 1) it incorporated a lysine moiety for water solubility, 2) it contained three consecutive guanine units that could each be part of a different G tetrad, and 3) the acridone was linked to PNA by a flexible linker and can therefore stack favorably with the top G tetrad of the hybrid quadruplex once formed. Compound **1** was synthesized on rink amide 4-methylbenzhydrylamine (MBHA) resin (Merck Biosciences) using standard (9*H*-fluoren-9-ylmethoxy)carbonyl (Fmoc) chemistry. The structure of the acridone was based on the bis(aminoalkylamido)acridone quadruplex ligands[17] and was attached to the PNA by a glycine linker. The acridone monomer **6** was synthesized in solution in six steps that required no purification on silica gel (Scheme 2).

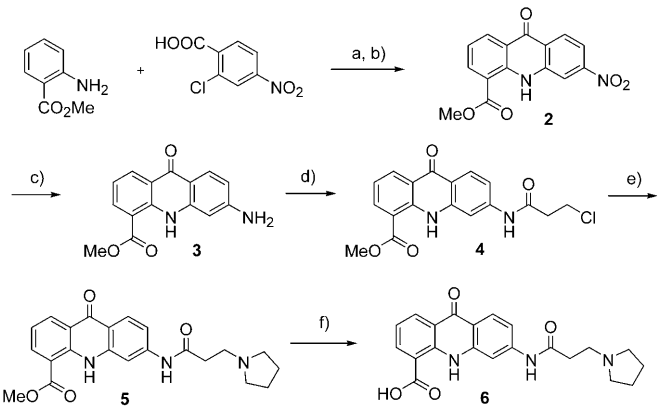

Scheme 2. Synthesis of the acridone carboxylic acid building block **6**. Reagents and conditions: a) Cu, Cu_2O, $Cu(OAc)_2$, DMF, 160 °C, 1 h (50%); b) PPA, 130 °C, 45 min (85%); c) $SnCl_2{\cdot}2H_2O$, AcOH, HCl, 15 min, RT, then 45 min, 80 °C (66%); d) 3-CPC, 60 °C, 24 h (85%); e) pyrrolidine, DMF, 60 °C, 30 min (92%); f) NaOH, H_2O, DMF, 50 °C, 40 min (89%). DMF = *N*,*N*-dimethylformamide, PPA = polyphosphonic acid, 3-CPC = 3-chloropropionyl chloride.

The Ullman reaction between commercially available methyl anthranilate and 2-chloro-5-nitrobenzoic acid by using a modified version of a previously reported protocol[18] afforded the bis(aryl)amine, which was almost quantitatively converted into the corresponding acridone **2** after treatment in polyphosphoric acid and precipitation in water. Reduction of the nitro group with tin(II) chloride under acidic conditions afforded the amino acridone **3**, which was treated with 3-chloropropionyl chloride to form the corresponding acridone amide **4**. Nucleophilic addition of pyrrolidine on the aliphatic halide generated the desired 3-pyrrolidine proprionamide-substituted acridone methyl ester **5**, which was

finally hydrolyzed under basic conditions to afford the desired acridone carboxylate **6**.

Characterization of a DNA_1/PNA_1 quadruplex: By using a combination of UV, circular dichroism (CD), and fluorescence spectroscopic and mass-spectrometric analysis, we have established the interactions between a three-repeat fragment of human telomeric DNA d(GGGTTAGGGTTAGGG) **G3** and the PNA–acridone **1**. Fragment **G3** formed a stable quadruplex ($T_m = 59.5\,°C$) in potassium phosphate buffer (100 mM, pH 7.4 also containing 100 mM KCl) at a strand concentration of 20 μM. Fragment **G3** exhibited a CD signature with two maxima at 260 and 295 nm characteristic of a mixture of parallel and antiparallel G-quadruplex conformations, respectively. When annealed in the presence of an equimolar amount of PNA **1**, the UV thermal denaturation curve showed a melting transition at $T_m = 60.5\,°C$, only one degree higher than for the DNA alone (Table 1). However the CD profile was significantly different with a main maximum at $\lambda = 260$ nm and a smaller one at $\lambda = 295$ nm (Figure 1), thus indicting either 1) a ligand-induced conformational switch of the dimeric DNA quadruplex or 2) the formation of an alternative hybrid PNA–DNA quadruplex structure that accounts for the new CD signature.

Table 1. Melting temperatures of DNA (20 μM **G3**) and DNA/PNA (20 μM **G3**+20 μM PNA **1**) in buffers containing different potassium concentrations.

Buffer composition	Complex	T_m [°C]	ΔT_m [°C][a]
100 mM KH_2PO_4 pH 7.4+100 mM KCl	**G3**	59.5	+1
	G3+PNA **1**	60.5	
100 mM KH_2PO_4 pH 7.4	**G3**	51.0	+4
	G3+PNA **1**	55.0	
H_20 pH 7.4	**G3**	<10	>+13
	G3+PNA **1**	23.0	

[a] Difference in T_m values obtained under identical conditions for the solutions of 20 μM **G3**+20 μM PNA **1** and 20 μM **G3**.

Similar CD and UV spectroscopic experiments were carried out but with decreasing concentrations of salt (either in 100 mM potassium phosphate buffer with no added KCl first or in neat water at controlled pH 7.4). As expected for the 20 μM solution of **G3**, the T_m value decreased significantly on lowering the potassium concentration: the T_m value went from 59.5 to 51 °C on removing the additional 100 mM KCl of the initial potassium phosphate buffer, and $T_m < 10\,°C$ when annealed in neat water (Table 1). A salt-dependent shift in the T_m values was also observed for the equimolar PNA/DNA mixture: the T_m value went from 60.5 to 55 °C with no added KCl and $T_m = 23\,°C$ in neat water (Table 1). Interestingly, the difference in the T_m values between **G3** alone and **G3**+1 equiv PNA **1** gradually increases on decreasing the salt concentration.

Cation-mediated stabilization of DNA quadruplexes is mainly through 1) electrostatic screening of the negatively charged DNA strands and 2) coordination of the eight O6

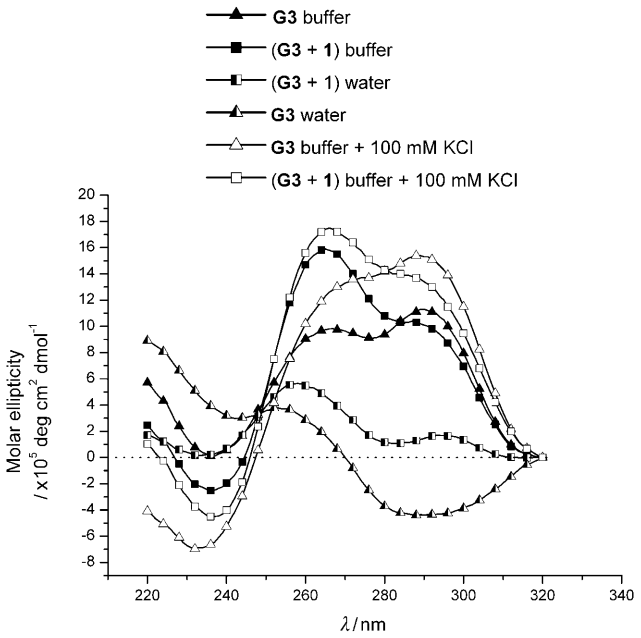

Figure 1. CD spectra of solutions of 20 μM **G3** and 20 μM **G3**+20 μM PNA **1** annealed in either potassium phosphate buffer 100 mM at pH 7.4 containing 100 mM KCl (empty triangles and squares), potassium phosphate buffer 100 mM at pH 7.4 (full triangles and squares) or neat water at pH 7.4 (half-full triangles and squares).

functional groups on the guanine units between the tetrads.[19] Contrary to this behavior, noncovalent PNA complexes were shown to be slightly destabilized by cations[20] and the previously reported PNA_4 quadruplex showed comparable stability when annealed either in neat water or 100 mM sodium phosphate buffer.[12] Herein, we demonstrate that the PNA/DNA complex is stabilized by potassium cations, although not as strongly as a pure DNA quadruplex. It is also noteworthy that in experiments carried out with stoichiometric mixtures of **G3** and acridone **6** that lack the PNA strand, no thermal stabilization or structural changes of the quadruplex were observed (data not shown). This finding rules out the possibility of a conformational change of the **G3** dimeric quadruplex induced by the acridone only and reinforces the initial hypothesis of an active participation of the PNA in PNA–DNA hybrid quadruplex formation.

CD spectroscopic experiments were also carried out on **G3** and **G3**/PNA **1** complexes annealed either in potassium phosphate buffer (with or without 100 mM KCl) or neat water at pH 7.4 (Figure 1). Fragment **G3** formed a mixed parallel/antiparallel quadruplex in potassium phosphate buffer but remained unstructured when annealed in neat water, which is consistent with the reported data.[3] When annealed in the presence of an equimolar amount of PNA **1**, **G3** formed a mixed parallel/antiparallel quadruplex in potassium phosphate buffer and neat water, which is consistent with the UV/melting experiments that demonstrated that PNA **1** could induce the formation of a quadruplex even under conditions in which the dimeric DNA quadruplex

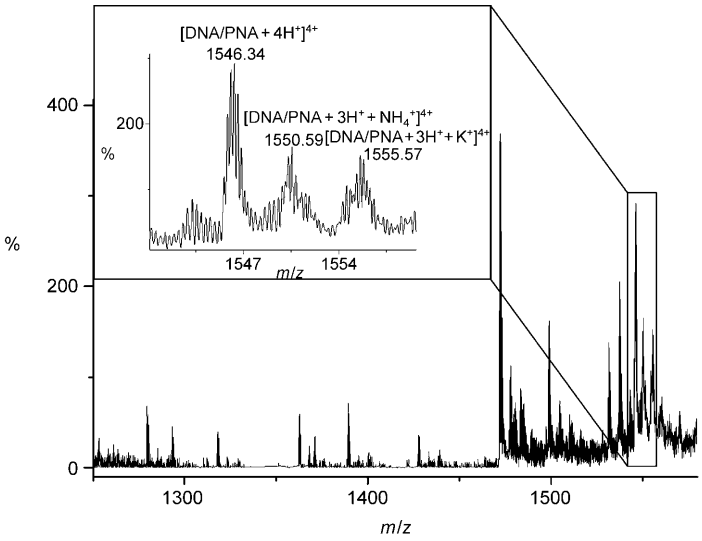

Figure 2. Nano ESI mass spectrum of an equimolar solution of DNA **G3** and PNA **1** annealed in ammonium acetate buffer.

cannot form. Interestingly, 1) the absolute amount of quadruplex formed decreased on decreasing the salt concentration, 2) the ratio of emissions at $\lambda = 260/295$ nm in the CD spectra remains almost constant for either the **G3** or **G3**/PNA **1** complex whatever the buffer, and 3) this ratio remains significantly higher for the PNA/DNA quadruplex than for the pure DNA quadruplex. Taken all together, these CD and UV spectroscopic data confirm that **G3** forms a stable mixed parallel/antiparallel quadruplex structure, the stability of which is highly dependent on the salt concentration. When annealed with a stoichiometric amount of PNA **1**, **G3** also folds into a quadruplex, but with a different conformation (more parallel-like), and the stability of this new quadruplex is significantly less influenced by the salt concentration. This outcome is consistent with the formation of a hybrid PNA/DNA quadruplex with a participation of the PNA guanine units into mixed tetrads with the guanine moieties of the **G3** DNA strand. The difference in the CD spectra between the pure DNA and hybrid PNA/DNA quadruplex could be explained by an acridone-induced orientation of the PNA strand. Indeed, whereas in the dimeric DNA quadruplex the lagging strand that participates in only a quarter of each G tetrad can freely and equally orientate in either way (all three guanine units are in a *syn* or *anti* conformation), it is anticipated that the acridone will preferentially bind to the most polar face of a quadruplex, and by this means will direct the positioning of the PNA with respect to the DNA strand. Indeed, it was previously reported that as a consequence of the position of the loops, quadruplexes often have one face rich in negative-charge potential whereas the other is more hydrophobic.[21] Given that the acridone possesses a positively charged side chain it is likely that it will preferentially interact with the most polar face.

To determine the stoichiometry of this quadruplex, we performed nano-electospray ionization mass spectrometry (nano ESI-MS) on a mixture of DNA **G3** and PNA **1**. The nano ESI mass spectrum showed multiple equidistant peaks in the regime m/z 1540–1560 (Figure 2). The peak centred at m/z 1546.2 showed fine structure (Figure 2, inset) with a constant separation of 0.25 ± 0.01, which indicates that the peaks in this regime correspond to a quadruply charged species. The associated molecular weight of this species ($M_W = 6181.5 \pm 2.5$ Da) corresponds to a bimolecular complex that is composed of one DNA strand and one PNA strand (calculated molecular weight = 6181.6 Da). Moreover, the family of peaks in this regime centred at m/z 1550.59 and 1555.57 corresponded to the same complex associated with one NH_4^+ and one K^+ cation, respectively. These results confirm the formation of a (3+1) hybrid PNA_1–DNA_1 quadruplex.

To delineate the ability of acridone-bearing PNA **1** to efficiently target such three G repeat sequences, its binding with the former was further investigated. Quadruplex ligands such as quinacridines[22] or carbazoles[23] exhibit changes in their fluorescent properties upon quadruplex binding that efficiently report on their DNA binding affinity and/or binding mode. Fluorescently labeled nucleic acid probes that are capable of detecting DNA single-base mismatches were recently reported that exploit the fact that the fluorescence of the intercalator is directly responsive to local perturbations that arise upon hybridization of the probe to the DNA target.[24] In these systems, interaction of the fluorophore with G bases or G–C base pairs often result in a significant quenching of fluorescence.

The emission of fluorescence of a solution of PNA **1** was recorded under different conditions to ascertain whether indeed the acridone moiety behaved as a quadruplex binding ligand (Figure 3). When 3 μM PNA **1** was annealed with 3 μM DNA **G3** under quadruplex forming conditions, a palpable increase in the fluorescence intensity (≈40%) was observed. This fluorescence enhancement was also accompanied by a moderate red shift from $\lambda = 431$ to 436 nm. However, when 3 μM PNA **1** was incubated with 3 μM ssDNA (of sequence similar to that of **G3** but carrying three G→T mutations to prevent quadruplex formation), it did not lead to any significant changes in the fluorescence properties of the acridone moiety. This result is consistent with a specific interaction of PNA **1** with **G3** that additionally incorporates a stacking mode of the acridone moiety on a quadruplex core. Indeed, whereas in the case of PNA **1** the fluorescence of the acridone is likely to be quenched by free neighboring G bases, a structuration of PNA **1** within a quadruplex conformation, and of the three free guanine units in G-tertad formation could prevent such quenching and account for the observed fluorescence exhaltation.

To further investigate the nature of the binding interaction between PNA **1** and the DNA fragment **G3**, we first titrated a solution of **1** (3 μM) with increasing amounts of **G3** prefolded into the quadruplex form as confirmed by CD spectroscopic analysis. This procedure resulted in a gradual decrease in the fluorescence intensity of the acridone moiety. Interestingly, when the same experiment was performed with increasing amounts of **G3** in the unfolded

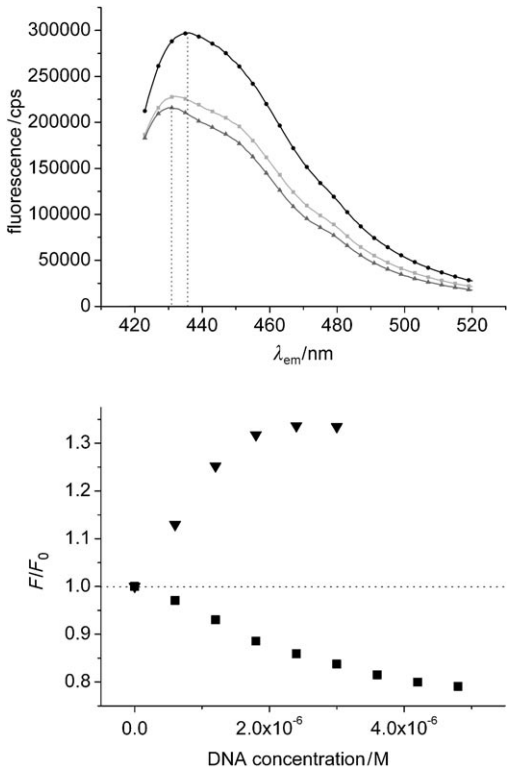

Figure 3. Top: fluorescence emission spectra ($\lambda_{ex}=410$ nm) of 3 μM PNA (dark-grey triangles), 3 μM PNA+3 μM ssDNA (pale grey squares), and 3 μM PNA+3 μM **G3** DNA (black circles) in 100 mM potassium phosphate buffer at pH 7.4 containing 100 mM KCl. Bottom: plots of F/F_0 (F=fluorescence intensity) versus the concentration of DNA **G3** for the titration of a 3 μM solution of PNA **1** in potassium phosphate buffer 100 mM at pH 7.4 containing 100 mM KCl with a solution of annealed **G3** (black squares) or unstructured **G3** (black triangles). Excitation was at $\lambda=410$ nm and emission was recorded at $\lambda=436$ nm.

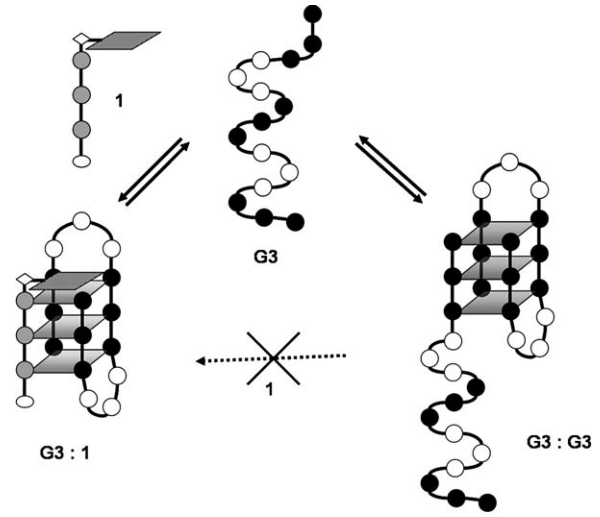

Scheme 3. Proposed modes of interaction of PNA **1** with **G3** DNA.

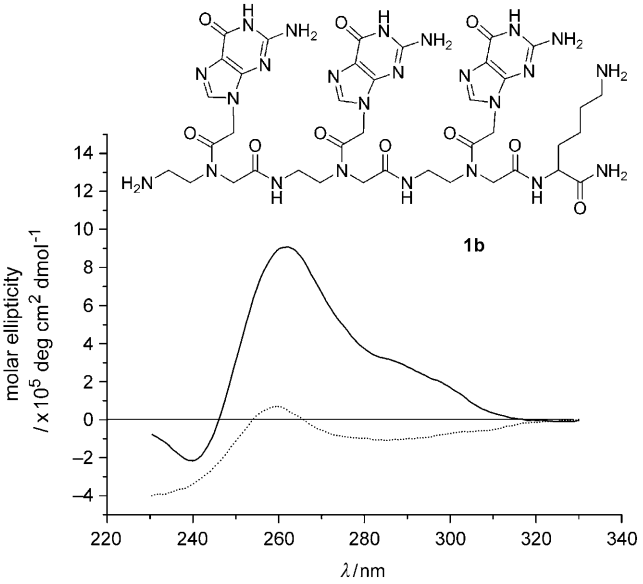

Figure 4. Structure of PNA **1b** and CD spectra of a stoichiometric mixture of (20 μM **G3**+20 μM PNA **1b**) annealed in either in potassium phosphate buffer 100 mM at pH 7.4 (full line) or water at pH 7.4 (dotted line).

single-stranded state it led to a significant increase in acridone fluorescence (Figure 3). Additionally, when a fixed amount of PNA **1** was annealed with increasing amounts of DNA **G3** an increase in fluorescence intensity was observed (data not shown) similar to that seen for the unfolded DNA **G3** (Figure 3). These results reflect two different binding modes for **1** on interacting with either a preformed quadruplex or a quadruplex forming sequence in the single-stranded state. Unlike nonfunctionalized G-rich PNA, PNA **1** is not capable of invading the dimeric quadruplex of **G3** once formed within the timescales investigated. However, it is capable of inducing G-rich single-stranded DNA folding into a quadruplex conformation even at room temperature and in neat water, thus leading to a thermodynamically favored hybrid structure (Scheme 3).

To demonstrate the influence of the acridone moiety on both the stability and conformation of the complex formed between PNA **1** and **G3**, an analogue of **1** that lacks the acridone platform, PNA **1b** (of general sequence Lys-GGG-NH_2), was synthesized (Figure 4). The ability of **1b** to form a stable bimolecular quadruplex upon binding to DNA **G3** was investigated using both UV and CD spectroscopic analysis in either 100 mM potassium phosphate buffer (pH 7.4) with no added KCl or neat water (pH 7.4). A stoichiometric mixture of PNA **1b** and DNA **G3** formed a stable quadruplex ($T_m=52.5$ °C) in 100 mM potassium phosphate buffer that was slightly more stable than the **G3** dimeric quadruplex (+1.5 °C) but less stable than the bimolecular hybrid quadruplex formed from PNA **1** and **G3** (−2.5 °C) under similar conditions. The CD spectrum of this new hybrid **1b**/**G3** quadruplex revealed a mixed parallel/antiparallel conformation with a main maximum at $\lambda=260$ nm (Figure 4), as previously observed with PNA **1**. More striking is the observation that PNA **1b** (which lacks the acridone platform) proved unable to form a hybrid PNA/DNA quadruplex in

the absence of any salt, unlike that observed with PNA acridone conjugate **1** (Figure 4). This observation along with the differences in T_m values measured in phosphate buffer demonstrates the influence of the acridone moiety on the stability of the hybrid quadruplex formed.

Interaction of PNA 1 with duplex DNA: The ability of the PNA acridone conjugate to stabilize double-stranded DNA was also examined using UV and fluorescence spectroscopic analysis. PNA binding to double-stranded DNA can happen through different binding modes. For example, one PNA strand can interact with two complementary DNA strands to form a PNA–DNA triplex or can also lead to duplex invasion with the formation of a PNA–DNA heteroduplex. Such an invasion has been demonstrated using a homopurine PNA decamer that only forms a duplex with the complementary oligonucleotides.[25] Herein, we investigated the capacity of our PNA **1** to either invade or associate with two B-DNA undecamers containing either a CCC motif complementary to the GGG PNA sequence (duplex B) or no sequence complementarity with PNA **1** (duplex A).

UV thermal denaturation experiments were carried out on duplexes A and B alone and with a stoichiometric amount of PNA **1**. Melting temperatures (T_m) of 53 °C were obtained for both duplexes A and B. Interestingly, no shift in the T_m values was observed on incubating either duplex A or B with PNA **1**, thus suggesting that our GGG PNA acridone conjugate cannot invade and stabilize B-DNA, even if the latter contains a CCC complementary sequence (Figure 5). To further investigate the specificity of PNA **1** toward quadruplex versus double-stranded DNA, additional UV thermal denaturation studies were carried out under low salt conditions (i.e., 10 mM potassium phosphate buffer, pH 7.4 and no added salt). Conditions employing low salt concentrations were previously reported to favor PNA binding to double-helix DNA.[26] Under those conditions, duplex B proved moderately stable (T_m = 36 °C). When incubated with a stoichiometric amount of PNA **1**, duplex B showed a similar melting temperature of 36 °C, indicative again of an absence of PNA-induced B-DNA stabilization. It is also noteworthy that 1) most PNA moieties commonly designed to invade duplex DNA and therefore interfere with DNA transcription are significantly longer than PNA **1** and 2) hybridization of **1** with a single strand of DNA containing a complementary CCC motif (i.e., ACG*CCC*TAAGC) did not lead to the formation of stable hybrid PNA/DNA duplexes or triplexes.

On titrating in a solution of **1** (3 μM) with increasing amounts of B-DNA, a decrease in the fluorescence intensity of the acridone was observed, which is comparable to that observed for the titration with a solution of folded **G3** quadruplex (Figure 5). This finding is consistent with our previous model that the nonspecific interaction of PNA **1** with either prefolded quadruplex or duplex DNA results in fluorescence quenching, whereas only the specific involvement of the PNA guanine units in G-tetrad formation leads to a significant fluorescence enhancement.

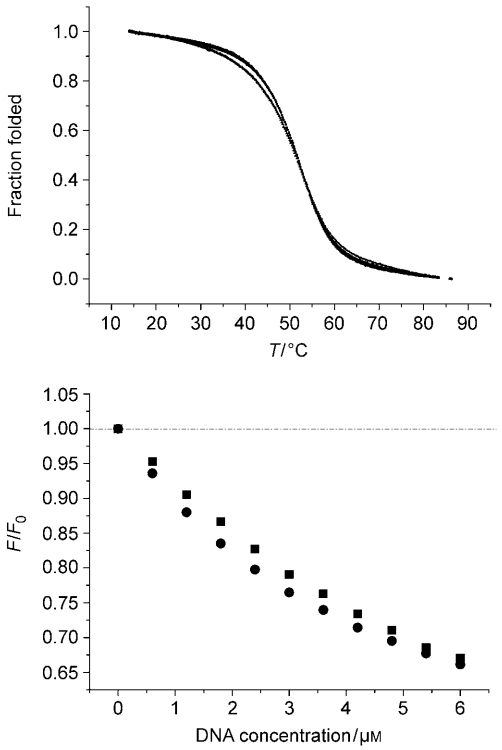

Figure 5. Top: Virtually superposed UV thermal denaturation curves (heating curve) of 4 μM duplex A, 4 μM duplex A + 4 μM PNA **1**, 4 μM duplex B, and 4 μM duplex B + 4 μM PNA **1**. Buffer was potassium phosphate buffer 100 mM at pH 7.4 containing 100 mM KCl. Bottom: plots of F/F_0 versus B-DNA concentration for the titration of a 3 μM solution of PNA **1** in potassium phosphate buffer 100 mM at pH 7.4 containing 100 mM KCl, with a solution of either noncomplementary duplex A (squares) or complementary duplex B (circles). Excitation was at λ = 410 nm and emission was recorded at λ = 436 nm.

Conclusion

We have reported a novel approach to target the human telomeric DNA sequence that combines a hybridization and an intercalation motif within a single scaffold. We have shown that this strategy is successful and have characterized the resultant (3 + 1) hybrid PNA_1/DNA_1 quadruplex, which is the first of a new genre of hybrid quadruplexes that also mimics one of the biologically relevant structures of the human telomeric quadruplex. The hybrid PNA–DNA bimolecular quadruplex showed increased stability at low salt concentration relative to the corresponding DNA_2 dimeric quadruplex. These studies open up new possibilities for the next generation of quadruplex ligands that target not only the external features of the quadruplex but also its central core constituted by the tetrads themselves. The absence of PNA-induced B-DNA stabilization also reinforces the potential of such conjugates as quadruplex specific ligands. However, because of the inability of PNA **1** to invade a dimeric quadruplex by displacement of one DNA strand, PNAs with increased affinity will be necessary before such quadruplex targeting strategy can be used in vivo. The design of second generation ligands containing two quadru-

plex binding platforms at both ends of the PNA strand that could significantly improve the stability of the hybrid quadruplex are currently being developed. Considering the increasing interest in DNA quadruplexes as either therapeutic targets in biology or supramolecular objects in nanosciences, ligands that can target DNA sequences containing only three clusters of guanine units, even under conditions in which DNA quadruplexes cannot readily form (low salt concentration), could be highly valuable.

Experimental Section

^{1}H and ^{13}C NMR spectra were recorded by using a Bruker Avance DRX 400 spectrometer at 400 and 100.6 MHz, respectively. Chemical shifts are reported as δ values (ppm) with reference to the residual solvent peaks. All the reagents and solvents were obtained from commercial sources and used without further purification. Purification of PNA acridone conjugate **1** was performed using a Gilson HPLC using a reverse-phase C_{18} column with gradients combining buffers A and B: buffer A = H_2O + 0.1% trifluoroacetic acid (TFA)); buffer B = (MeCN + 0.1% TFA).

2-{[2-(Methoxycarbonyl)phenyl]amino}-*para*-nitrobenzoic acid:[17] A mixture of 2-chloro-*para*-nitrobenzoic acid (5 g, 25 mmol), methyl anthranilate (5 g, 33 mmol), copper powder (190 mg, 3 mmol), Cu_2O (140 mg, 1 mmol), and $Cu(OAc)_2$ (360 mg, 2 mmol) were stirred at 160 °C in DMF (120 mL) for 3 h and then allowed to slowly warm to room temperature. After filtration through a thin layer of silica between two layers of celite, the addition of aqueous 0.1 M HCl (120 mL) and vigorous stirring led to the formation of an orange precipitate. The desired product was obtained as an orange solid (4 g) by filtration and used for the subsequent step without further purification (50%). ^{1}H NMR ([D$_6$]DMSO, 400 MHz): δ = 8.15 (br m, 2H), 7.98 (d, J = 7.6 Hz, 1H), 7.67 (d, J = 7.8 Hz, 1H), 7.66 (s, 1H), 7.60 (t, J = 7.8 Hz, 1H), 7.17 (t, J = 7.6 Hz, 1H), 3.88 ppm (s, 3H).

Methyl-3-nitro-acridone-5-carboxylate (2):[17] A mixture of 2-{[2-(methoxycarbonyl)phenyl]amino}-*para*-nitrobenzoic acid (1 g, 3.2 mmol) and polyphosphoric acid (10 g) was heated at 130 °C for 45 min. Water was added after cooling to room temperature, which led to the formation of a bright-yellow solid. The solid was removed by filtration, washed with water, and dried under vacuum. The acridone compound was obtained as a yellow solid (0.8 g, 85%). ^{1}H NMR ([D$_6$]DMSO, 400 MHz): δ = 9.02 (s, 1H), 8.55 (d, J = 7.2 Hz, 1H), 8.47 (d, J = 7.2 Hz, 1H), 8.41 (d, J = 8.4 Hz, 1H), 8.02 (d, J = 8.4 Hz, 1H), 7.44 (t, J = 7.2 Hz, 1H), 4.03 ppm (s, 3H).

Methyl-3-aminoacridone-5-carboxylate (3):[17] A mixture of **2** (1 g, 3.4 mmol), tin(II) chloride (3 g), and concentrated HCl (5 mL) was stirred vigorously for 20 min in glacial AcOH (20 mL). The reaction mixture was heated at 80 °C for 40 min and cooled to room temperature before water (80 mL) was added to allow the amino acridone to precipitate. After filtration and subsequent washes with ethyl acetate and diethyl ether, the desired product was obtained pure as a yellow powder (0.6 g, 66%). ^{1}H NMR ([D$_6$]DMSO, 400 MHz): δ = 8.46 (dd, ^2J = 8 Hz, ^3J = 1.8 Hz, 1H), 8.33 (dd, ^2J = 8 Hz, ^3J = 1.8 Hz, 1H), 7.93 (d, J = 8 Hz, 1H), 7.28 (t, J = 8 Hz, 1H), 6.62 (dd, ^2J = 8 Hz, ^3J = 1.8 Hz, 1H), 6.54 (d, J = 1.8 Hz, 1H), 3.98 ppm (s, 3H); HRMS: m/z calcd for $C_{15}H_{13}N_2O_3^+$: 269.0921; found: 269.0914.

Methyl-3-(3-chloropropionamide)-acridone-5-carboxylate (4): A suspension of **3** (0.5 g, 1.9 mmol) in 3-chloropropionyl chloride (20 mL) was heated at 60 °C for 24 h. The product precipitated at room temperature by the addition of diethyl ether and was collected by filtration. The resulting dark-yellow powder was washed with ethyl acetate, water, and diethyl ether, thus affording the desired product pure as a pale-brown solid (0.6 g, 85%). ^{1}H NMR ([D$_6$]DMSO, 400 MHz): δ = 7.61 (d, J = 8.4 Hz, 1H), 7.47 (d, J = 8 Hz, 1H), 7.32 (s, 3H), 7.26 (d, J = 8.4 Hz, 1H), 6.44 (t, J = 8 Hz, 1H), 6.40 (d, J = 8 Hz, 1H), 3.08 (s, 3H), 3.02 (t, J = 6 Hz, 4H), 2.03 ppm (t, J = 6 Hz, 2H); ^{13}C NMR (DMSO, 100 MHz): δ = 176, 169.5, 168, 144.5, 141.4, 141.3, 136.5, 133, 127.5, 122, 120.5, 117, 115.2, 114.8, 106.4, 53.2, 41, 24 ppm; HRMS: m/z calcd for $C_{18}H_{15}ClLiN_2O_4^+$: 365.0875; found: 365.0861.

Methyl-3-[3-(pyrrolidin-1-yl)propanamido]-acridone-5-carboxylate (5): Pyrrolidine (500 μL, 5.6 mmol) was added to a solution of **4** (0.5 g, 1.4 mmol) in DMF (2.5 mL). The reaction mixture was stirred at 60 °C for 30 min until the reaction had gone to completion. After cooling to room temperature, diethyl ether was added to precipitate a yellow solid. After recrystallization from diethyl ether, the desired product was obtained pure as a yellow solid (0.5 g, 92%). ^{1}H NMR ([D$_6$]DMSO, 400 MHz): δ = 8.54 (d, J = 7.8 Hz, 1H), 8.42 (d, J = 7.8 Hz, 1H), 8.20 (s, 1H), 8.20 (d, J = 7.8 Hz, 1H), 7.39 (t, J = 7.8 Hz, 1H), 7.38 (d, J = 7.8 Hz, 1H), 4.00 (s, 3H), 3.47 (t, J = 6 Hz, 2H), 1.85 (t, J = 6 Hz, 2H), 3.10 (br m, 4H), 1.97 ppm (br m, 4H); ^{13}C NMR ([D$_6$]DMSO, 100 MHz): δ = 176, 169.5, 168, 144.5, 141.4, 141.3, 136.5, 133, 127.5, 122, 120.5, 117, 115.2, 114.8, 106, (53.5, 2C), 53.2, 50, 33 ppm (23, 2C); HRMS: m/z calcd for $C_{22}H_{24}N_3O_4^+$: 394.1761; found: 394.1789.

Sodium-3-[3-(pyrrolidin-1-yl)propanamido]-acridone-5-carboxylate (6): An aqueous solution of NaOH (0.96 mL, 1 M, 1.5 equiv) was added to a solution of **5** (0.25 g, 0.64 mmol) in DMF (10 mL). The reaction mixture was stirred at 50 °C for 40 min. After removal of the water through evaporation, diethyl ether was added. The resulting precipitate was collected by filtration and triturated with diethyl ether until a yellow solid was obtained. The solid was washed with ethyl acetate and diethyl ether, thus leading to the desired carboxylate acridone pure as a light-yellow solid (0.23 g, 89%). ^{1}H NMR (D_2O, 400 MHz): δ = 7.88 (d, J = 7.2 Hz, 1H), 7.72 (d, J = 7.2 Hz, 1H), 7.18 (d, J = 8.8 Hz, 1H), 6.85 (t, J = 7.2 Hz, 1H), 6.51 (s, 3H), 6.17 (d, J = 8.8 Hz, 1H), 2.64 (t, J = 7.2 Hz, 2H), 2.55 (br m, 4H, brm), 2.20 (t, J = 7.2 Hz, 2H), 1.73 ppm (br m, 4H); ^{13}C NMR (D_2O, 100 MHz): δ = 177, 173, 171, 141.5, 140, 139, 136, 129, 126, 120.5, 119.9, 119.8, 115, 113.5, 104, (53.5, 2C), 50, 35 ppm (23, 2C); HRMS: m/z calcd for $C_{21}H_{22}N_3O_4^+$: 380.1605; found: 380.1616.

MALDI-TOF spectra of PNA 1 and 1b: PNA **1** and **1b** were synthesized on a solid support using Fmoc chemistry. The PNA strand was cleaved from the resin with a 95% TFA solution and purified by HPLC. The final compounds were characterized by HRMS (MALDI-TOF): PNA **1**: m/z: calcd for $C_{62}H_{77}N_{28}O_{14}$: 1437.617; found: 1437.675 $[M+H]^+$. PNA **1b**: m/z: calcd for $C_{39}H_{55}N_{24}O_{10}$: 1019.446; found: 1019.542 $[M+H]^+$.

DNA oligonucleotide preparation: All oligonucleotides were purchased from Sigma Genosis. All concentrations were expressed in strand molarity with a nearest-neighbor approximation for the absorption concentrations of the unfolded species. The DNA and hybrid PNA: DNA quadruplexes were prepared in 100 mM potassium phosphate buffer containing 100 mM KCl at pH 7.4. After heating to 95 °C for 5 min, the solution was slowly cooled for 6 h to room temperature and the oligonucleotide solutions were finally stored at 4 °C.

Oligonucleotide sequences: **G3** d(GGGTTAGGGTTAGGG), ssDNA d(GTGTTAGTGTTAGTG), duplex A d(GCATAGTGCGT) hybridized with its complementary sequence, and duplex B d(GCTTAGGGCGT) hybridized with its complementary sequence.

Fluorescence spectroscopy: Fluorescence emission spectra were recorded in quartz cells at 20 °C by means of a Jobin Yvon Fluorolog 3.22 instrument. The excitation and emission bandwidths were fixed to 5 and 5 nm, respectively. Fluorescence titration experiments were carried out by using a 500-μL quartz cuvette containing a solution of 3 μM PNA–acridone conjugate **1** in 100 mM potassium phosphate buffer containing 100 mM KCl (pH 7.4). Concentrated DNA aliquots (from a 150 μM stock solution) were directly added to the PNA solution. The spectra were recorded between $\lambda = 420$ and 520 nm while exciting at 410 nm.

UV spectroscopy: Absorption spectra were recorded by using a Uvicon XL spectrophotometer. Quadruplex and duplex DNA melting curves were recorded at wavelengths of $\lambda = 295$ and 260 nm, respectively, between 15 and 90 °C at 0.5 °C min^{-1}. For quadruplex melting, the DNA (and PNA when appropriate) concentration was 20 μM. For duplex melting, the DNA (and PNA when appropriate) concentration was 4 μM.

CD spectroscopy: CD spectra were recorded by using a Jobin-Yvon spectrophotometer in a 2 mm pathlength cuvette (300 μL). Spectra were recorded at 25 °C from $\lambda = 320$ to 220 nm and are presented at an average of three successive scans. Finally, all the spectra were subtracted from a baseline corresponding to the buffer alone (100 mM potassium phosphate buffer containing 100 mM KCl) when appropriate.

Nano ESI-MS: All mass-spectrometric measurements were performed by using a Micromass ESI-MS Q-TOF Ultima Mass Spectrometer (Manchester, UK) with microchannel plate detector. Noncovalent nano ESI-MS spectra were collected in positive-ion mode for the PNA–DNA complex and the negative-ion mode for the sample containing DNA alone. A 1:1 PNA/DNA solution with a strand concentration of 1 mM, prepared in 150 mM ammonium acetate buffer (pH 7) was heated to 95 °C, annealed to room temperature over 3 h, and equilibrated at 4 °C overnight. A 500 μM solution containing DNA was also prepared similarly. Just prior to injection, the equilibrated DNA/PNA complex was diluted fivefold with isopropanol/water (1:4). The solution of DNA was similarly diluted fivefold with methanol/water (1:4) The source parameters employed during acquisition of the mass spectra: source temperature: 20 °C; capillary voltage: 2 and −2.23 kV for the PNA/DNA and DNA complexes, respectively; cone voltage: 70 V.

Acknowledgement

The authors thank the "Centre National pour la Recherche Scientifique" (CNRS) (S.L.), the "Ministère de la Recherche et de l'Enseignement Supérieur" (A.P.), and CSIR, Government of India, (P.S.) for financial support. Y.K. thanks DBT, Government of India for the Innovative Young Biotechnologist Award.

[1] G. N. Parkinson in Q *uadruplex Nucleic Acids*; (Eds.: S. Neidle, S. Balasubramanian), RSC Biomolecular Sciences Publishing, Cambridge **2006**, pp. 1–30.

[2] a) J. L. Huppert, S. Balasubramanian, S. *Nucleic Acids Res.* **2005**, *33*, 2908–2916; b) A. K. Todd, M. Johnston, S. Neidle, *Nucleic Acids Res.* **2005**, *33*, 2901–2907; c) J. Eddy, N. Maizels, *Nucleic Acids Res.* **2008**, *36*, 1321–1333.

[3] I. M. Pedroso, L. F. Duarte, G. Yanez, K. Burkewitz, T. M. Fletcher, *Biopolymers* **2007**, *87*, 74–84.

[4] D. J. Patel, A. T. Phan, V. Kuryavyi, *Nucleic Acids Res.* **2007**, *35*, 7429–7455.

[5] K. Paeschke, T. Simonsson, J. Postberg, D. Rhodes, H. J. Lipps, *Nat. Struct. Mol. Biol.* **2005**, *12*, 847–854.

[6] A. M. Zahler, J. R. Williamson, T. R. Cech, D. M. Prescott, *Nature* **1991**, *350*, 718–720.

[7] W. C. Hahn, S. A. Stewart, M. W. Brooks, S. G. York, E. Eaton, A. Kurachi, R. L. Beijersbergen, J. H. Knoll, M. Meyerson, R. A. Weinberg, *Nature Med.* **1999**, *5*, 1164–1170.

[8] For a recent review, see: D. Monchaud, M.-P. Teulade-Fichou, *Org. Biomol. Chem.* **2008**, *6*, 627–636.

[9] B. Datta, B. Armitage, *J. Am. Chem. Soc.* **2001**, *123*, 9612–9619.

[10] S. Ladame, J. A. Schouten, J. Roldan, J. E. Redman, S. Neidle, S. Balasubramanian, *Biochemistry* **2006**, *45*, 1393–1399.

[11] R. Rodriguez, G. D. Pantos, D. P. N. Gonçalvez, J. K. M. Sanders, S. Balasubramanian, *Angew. Chem.* **2007**, *119*, 5501–5503; *Angew. Chem. Int. Ed.* **2007**, *46*, 5405–5407.

[12] Y. Krishnan-Ghosh, E. Stephens, S. Balasubramanian, *J. Am. Chem. Soc.* **2004**, *126*, 5944–5945.

[13] B. Datta, C. Schmitt, B. A. Armitage, *J. Am. Chem. Soc.* **2003**, *125*, 4111–4118.

[14] S. Roy, F. A. Tanious, W. D. Wilson, D. H. Ly, B. A. Armitage, *Biochemistry* **2007**, *46*, 10433–10443.

[15] L. Petraccone, B. Pagano, V. Esposito, A. Randazzo, G. Piccialli, G. Barone, C. A. Mattia, C. Giancola, *J. Am. Chem. Soc.* **2005**, *127*, 16215–16223.

[16] N. Zhang, A. T. Phan, D. J. Patel, *J. Am. Chem. Soc.* **2005**, *127*, 17277–17285.

[17] R. J. Harrison, A. P. Reszka, S. M. Haider, B. Romagnoli, J. Morrell, M. A. Read, S. M. Gowan, C. M. Incles, L. R. Kelland, S. Neidle, *Bioorg. Med. Chem. Lett.* **2004**, *14*, 5845–5849.

[18] W. A. Denny, G. J. Atwell, B. C. Baguley, *J. Med. Chem.* **1983**, *26*, 1619–1625.

[19] C. C. Hardin, M. J. Corregan, D. V. Lieberman, B. A. Brown, *Biochemistry* **1997**, *36*, 15428–15450.

[20] S. Tomac, M. Sarkar, T. Ratilainen, P. Wittung, P. E. Nielsen, B. Nordén, A. Gräslund, *J. Am. Chem. Soc.* **1996**, *118*, 5544–5552.

[21] S. Ladame, J. A. Schouten, J. Stuart, J. Roldan, S. Neidle, S. Balasubramanian, *Org. Biomol. Chem.* **2004**, *2*, 2925–2931.

[22] M.-P. Teulade-Fichou, C. Carrasco, L. Guittat, C. Bailly, P. Alberti, J.-L. Mergny, A. David, J.-M. Lehn, W. D. Wilson, *J. Am. Chem. Soc.* **2003**, *125*, 4732–4740.

[23] C.-C. Chang, J.-Y. Wu, C.-W. Chien, W.-S. Wu, H. Liu, C.-C. Kang, L.-J. Yu, T.-C. Chang, *Anal. Chem.* **2003**, *75*, 6177–6183.

[24] C. Dohno, I. Saito, *ChemBioChem* **2005**, *6*, 1075–1081.

[25] E. Nielsen, L. Christensen, *J. Am. Chem. Soc.* **1996**, *118*, 2287–2288.

[26] H. J. Larsen, P. E. Nielsen, *Nucleic Acids Res.* **1996**, *24*, 458–463.

Received: April 1, 2008
Published online: July 30, 2008

